



1 Statistical Analysis for Satellite Index-Based Insurance to 2 define Damaged Pasture Thresholds

3

4 **Juan José Martín-Sotoca^{1*}, Antonio Saa-Requejo^{2,3}, Rubén Moratíel^{2,3}, Nicolas Dalezios⁴, Ioannis**
5 **Faraslis⁵, and Ana María Tarquis^{2,6}**

6 jmartinsotoca@gmail.com, antonio.saa@upm.es, ruben.moratíel@upm.es, dalezios.n.r@gmail.com,
7 faraslisgiannis@yahoo.gr, anamaria.tarquis@upm.es

8

9 ¹ Data Science Laboratory. European University, Madrid, Spain.

10 ² CEIGRAM, Research Centre for the Management of Agricultural and Environmental Risks, Madrid, Spain.

11 ³ Dpto. Producción Agraria. Universidad Politécnica de Madrid, Spain.

12 ⁴ Department of Civil Engineering. University of Thessaly, Volos, Greece.

13 ⁵ Department of Planning and Regional Development. University of Thessaly, Volos, Greece.

14 ⁶ Grupo de Sistemas Complejos. Universidad Politécnica de Madrid, Spain.

15

16 * Correspondence to: jmartinsotoca@gmail.com

17 **Abstract:** Vegetation indices based on satellite images, such as Normalized Difference Vegetation Index
18 (NDVI), have been used in countries like USA, Canada and Spain for damaged pasture and forage
19 insurance for the last years. This type of agricultural insurance is called “satellite index-based
20 insurance” (SIBI). In SIBI, the occurrence of damage is defined through NDVI thresholds mainly based
21 on statistics derived from normal distributions. In this work a pasture area at the north of Community
22 of Madrid (Spain) has been delimited by means of MODIS images. A statistical analysis of NDVI
23 histograms was applied to seek for the best statistical distribution using maximum likelihood method.
24 The results show that the normal distribution (NORMAL) is not the optimal representation and the
25 General Extreme Value (GEV) distribution presents a better fit through the year. A comparison
26 between NORMAL and GEV are showed respect to the probability under a NDVI threshold value along
27 the year. This suggests that a priori distribution should not be selected and a percentile methodology
28 should be used to define a NDVI damage threshold rather than the average and standard deviation,
29 typically of normal distributions.

30 **Keywords:** NDVI, pasture insurance, GEV distribution, MODIS.

31

32

Highlights

- 33 • **General Extreme Value (GEV) distribution provides the best fit to the NDVI**
34 **historical observations.**
- 35 • **Difference between Normal and GEV distributions are higher during spring**
36 **and autumn, transition periods in the precipitation regimen.**
- 37 • **NDVI damage threshold shows evident differences using Normal and GEV**
38 **distributions covering both the same probability (24.20%).**
- 39 • **NDVI damage threshold values based on percentiles calculation is proposed**
40 **as an improvement in the index based insurance in damaged pasture.**



41

42 **1. Introduction**

43 Agricultural insurance addresses the reduction of the risk associated with crop
44 production and animal husbandry. The concept of index-based insurance (IBI) attempts
45 to achieve settlements based on the value taken by an objective index rather than on a
46 case-by-case assessment of crop or livestock losses (Gommes and Kayitakier, 2013).
47 Indeed, the goal of IBI policy remains to develop an affordable tool to all producers,
48 including smallholders. Specifically, IBI can constitute a safety net against
49 weather-related risks for all members of the farming community, thereby increasing
50 food security and reducing the vulnerability of rural populations to weather extremes.
51 Moreover, IBI can be associated with credits for insured smallholders, due to the fact
52 that the risk of non-repayment for lenders is reduced, which encourages the use of
53 agricultural inputs and equipment, leading to increased and more stable crop
54 production. Over the past decade, the importance of weather index-based insurances
55 (WIBI) for agriculture has been increasing, mainly in developing countries (Gommes
56 and Kayitakier, 2013). This interest can be explained by the potential that IBI
57 constitutes a risk management instrument for small farmers. Indeed, it can be
58 considered within the context of renewed attention to agricultural development as
59 one of the milestones of poverty reduction and increased food security, as well as the
60 accompanying efforts from various stakeholders to develop agricultural risk
61 management instruments, including agricultural insurance products.

62

63 Farmers need to protect their land and crops specifically from drought in arid and
64 semi-arid countries, since their production may directly depend mainly on the impacts
65 of this particular natural hazard. Insurance for drought-damaged lands and crops is
66 currently the main instrument and tool that farmers can resort in order to deal with
67 agricultural production losses due to drought. Many of these insurances are using
68 satellite vegetation indices (Rao, 2010), thus they are also called “satellite index-based
69 insurances” (SIBI). SIBI have some advantages over WIBI, such as cost-effective
70 information and acceptable spatial and temporal resolution. They do not, however,
71 resolve the issue of basis risk, i.e. potential unfairness to insurance takers (Leblois,
72 2012). Moreover, the very nature of an index-based product creates the chance that
73 an insured party may not be paid when they suffer loss. For this reason, in some
74 countries (Spain) they have named this SIBI as “damaged in pasture” to cover not only
75 drought even this one is the main cause.

76

77 It is highly recognized that shortage of water has many implications to agriculture,
78 society, economy and ecosystems. Specifically, its impact on water supply, crop
79 production and rearing of livestock is substantial in agriculture. Knowing the likelihood
80 of drought is essential for impact prevention (Dalezios, 2013). Drought severity



81 assessment can be approached in different ways: through conventional indices based
82 on meteorological data, such as temperature, rainfall, moisture, etc. (Niemeyer, 2008),
83 as well as through remote sensing indices based on images usually taken by artificial
84 satellites (Lovejoy et al., 2008) or drones. In the second group they are found Satellite
85 Vegetation Indices (SVI), which can quantify “green vegetation”, and soil moisture
86 through Soil Water Index (Gouveia et al., 2009) combining different spectral
87 reflectances. Thus, they are one of the main ways to quantitatively assess drought
88 severity.

89

90 At the present time, several satellites (NOAA, TERRA, DEIMOS, etc.) can provide
91 this spectral information with different spatial resolution. Some series with a high
92 temporal frequency are freely available, those from NOAA satellites and Terra. The
93 most widely known SVI is the Normalized Difference Vegetation Index (NDVI). It
94 follows the principle that healthy vegetation mainly reflects the near-infrared
95 frequency band. There are several other important SVI, such as Soil Adjusted
96 Vegetation Index (SAVI) and Enhanced Vegetation Index (EVI) that incorporate soil
97 effects and atmospheric impacts, respectively. An important point of this class of
98 insurance is “when damage occurs”. To measure this, a SVI threshold value is defined
99 mainly based on statistics that apply to normally distributed variables: average and
100 standard deviation. When current SVI values are below this threshold value for a
101 period of time, insurance recognizes that a damage is occurring, most of the times
102 drought, and then it begins to pay compensations to farmers.

103

104 WIBI aims to protect farmers against weather-based disasters such as droughts,
105 frosts and floods. A WIBI policy links possible insurance payouts with the weather
106 requirements of the crop being insured: the insurer pays an indemnity whenever the
107 realized value of the weather index meets a specified threshold. Whereas payouts in
108 traditional insurance programs are related to actual crop damages, a farmer insured
109 under a WIBI contract may receive a payout. A current difficulty to the wide
110 implementation of WIBI is the weakness of indices. Indeed, there is certainly a need for
111 more efficient indices based on the additional experience gained from the
112 implementation of WIBI products in the developing world. Current trends in index
113 technology are exciting and they actuate high expectations, especially the
114 development of yield indices and the use of remote sensing inputs. Risk protection and
115 insurance illiteracy constitute another difficulty, which has to be addressed by training
116 and awareness-raising at all levels, from farmers to farmers’ associations,
117 micro-insurance partners, as well as senior decision-makers in insurance, banking, and
118 politics (Bailey, 2013). It is essential that all stakeholders (especially the insured)
119 perfectly understand the principles of IBI, as otherwise the insurer, even the whole
120 concept of insurance, is at risk of reputation loss for years or decades.

121



122 There is currently a lack of technical capacity in the insurance sectors of most
123 developing countries, which is a constraint to the scaling up and further development
124 of WIBI (Gommes and Kayitakire, 2012). Specifically, although it is possible to design an
125 index product and assist in roll-out, marketing, and sales, such assistance is not
126 possible on a wide scale, simply because there is lack of qualified expertise. Indeed, it
127 usually requires mathematical modeling, data manipulation, and expertise in crop
128 simulation to design an index. Nevertheless, it is possible to structure insurance with
129 multiple indices, but this increases the complexity of the product and makes it difficult
130 for farmers to comprehend it. ‘Basis risk’ is also a particular problem for index
131 products, which is frequently caused by the fact that measurements of a particular
132 variable, such as rain, may differ at the insurer’s measurement site and in the farmer’s
133 field. This also creates problems for insurance providers. Indeed, part of the reason the
134 scaling up of index products has failed is that both insurers and farmers suffer from
135 this basis risk.

136

137 Currently, to mitigate impacts of climate-related reduced productivity of French
138 grasslands, several studies have been developed to design new insurance scheme
139 bases indemnity payouts to farmers on a forage production index (FPI) (Rumiguié et
140 al., 2015; 2017). Two examples of SIBIs are presented in two different countries: USA
141 and Spain. In particular, in USA there are several insurance programs for pasture,
142 rangeland and forage, which use various indexing systems (rainfall and vegetation
143 indices), and are promoted by Unites States Department of Agriculture (USDA) (Maples
144 et al., 2016; USDA, 2018). NDVI is the index chosen in the vegetation index program
145 and it is obtained from AVHRR (Advanced Very High Resolution Radiometer) sensor
146 onboard NOAA satellites. Average, maximum and minimum NDVI values are obtained
147 from a historical series with the aim of calculating a trigger value. Insurer decides the
148 quantity of compensation comparing this trigger with current value. On the other
149 hand, in Spain there exists the “Insurance for Damaged Pasture” from “Spanish System
150 of Agricultural Insurance” (BOE, 2013). This insurance defines damage event through
151 NDVI values obtained from MODIS (Moderate Resolution Imaging Spectroradiometer)
152 sensor onboard TERRA satellite of NASA. In this insurance, NDVI threshold values
153 ($NDVI_{th}$) are calculated subtracting several times ($k = 0.7$ or $k = 1.5$) standard deviation
154 to average within a homogeneous area:

155

$$156 \quad NDVI_{th} = \mu - k \cdot \sigma \quad (1)$$

157

158 where μ, σ are average and standard deviation of NDVI respectively. Average and
159 standard deviation come of supposing normal distributions in the historical data
160 (Goward et al., 1985; Hobbs, 1995; Fuller, 1998; Al-Bakri and Taylor, 2003; Turvey et
161 al., 2012; De Leeuw et al. 2014).

162



163 The aim of this paper is to find the best statistical NDVI distribution without the “a
164 priori” assumption that variables follow a Normal distribution, typically for current SIBI
165 methodology. In order to achieve this, the Maximum Likelihood Method (MLM) is
166 fitted to a historical series of NDVI values in a pasture land area in Spain (Community
167 of Madrid). Different types of distributions are examined with the aim of finding the
168 best fit. To eliminate some noise in the historical series, an original method is applied
169 consisting of using Hue-Saturation-Lightness (HSL) color model. Finally, Chi-square test
170 (χ^2 test) has been used to check the goodness of fit for all considered distributions.

171
172

173 **2. Materials and Methods**

174 **2.1 Vegetation Index**

175 The differences of the reflectance of green vegetation in parts of the
176 electromagnetic radiation spectrum, namely, visible and near infrared, provide an
177 innovative method for monitoring surface vegetation from space. Specifically, the
178 spectral behavior of vegetation cover in the visible (0.4-0.7mm) and near infrared
179 (0.74-1.1mm, 1.3-2.5mm) offers the possibility to monitor from space the changes in
180 the different stages of cultivated and uncultivated plants taking also into account the
181 corresponding behavior of the surrounding microenvironment (Ortega-Farias et al.,
182 2016). Indeed, from the visible part of the electromagnetic radiation spectrum it is
183 possible to draw conclusions about the rate photosynthesis, whereas from near
184 infrared inferences are extracted about the chlorophyll density and the amount of
185 canopy in the plant mass, as well as the water content in the leaves, which is also
186 linked directly to the rate of transpiration with impacts to physiological process of
187 photosynthesis. Usually, data from NOAA/AVHRR series of polar orbit meteorological
188 satellites are used with low spatial resolution (1.1 km²) and recurrence interval at least
189 twice daily from the same location. Several algorithms combining channels of red
190 (RED), near infrared (NIR) and green (GREEN) have been proposed, which provide
191 indices sensitive to green vegetation.

192

193 NDVI uses two frequency bands: red band (660 nm) and near-infrared band (860
194 nm). Absorption of red band is related to photosynthetic activity and reflectance of
195 near-infrared band is related to presence of vegetation canopies (Flynn, 2006). In
196 drought periods, NDVI values can reduce significantly, therefore many researchers
197 have used this index to measure drought events in recent years (Dalezios et al., 2014).
198 To calculate NDVI we will use this mathematical formula:

199

$$200 \quad NDVI = \frac{IR-R}{IR+R} \quad (2)$$



201
202 where IR and R are reflectance values in Near-Infrared band and Red band,
203 respectively. NDVI values below zero indicate no photosynthetic activity and are
204 characteristic of areas with large accumulation of water, such as rivers, lakes, or
205 reservoirs. The higher is the NDVI value, the greater is the photosynthetic activity and
206 vegetation canopies.

207
208 In this paper, the NDVI is used, which is widely known index with a multitude of
209 applications over time. The NDVI is suited for monitoring of total vegetation, since it
210 partly compensates the changes in light conditions, land slope and field of view (Kundu
211 et al., 2016). In addition, clouds, water and snow show higher reflectance in the visible
212 than in the near infrared, thus, they have negative NDVI values. Indeed, bare and rocky
213 terrain show vegetation index values close to zero. Moreover, the NDVI constitutes a
214 measure of the degree of absorption by chlorophyll in the red band of the
215 electromagnetic spectrum. In summary, the NDVI is a reliable index of the chlorophyll
216 density on the leaves, as well as the percentage of the leaf area density over land,
217 thus, NDVI constitutes a credible measure for the assessment of dry matter (biomass)
218 in various species vegetation cover (Dalezios, 2013). It is clear from the above that the
219 NDVI is an index closely related to growth and development of plants, which can
220 effectively monitor surface vegetation from space.

221
222 The continuous increase of the NDVI value during the growing season reflects the
223 vegetative and reproductive growth due to intense photosynthetic activity, as well as
224 the satisfactory correlation with the final biomass production at the end of a growing
225 period. On the other hand, gradual decrease of the NDVI values signifies stress due to
226 lack of water or extremely high temperatures for the plants, leading to a reduction of
227 the photosynthetic rate and ultimately a qualitative and quantitative degradation of
228 plants. NDVI values above zero indicate the existence of green vegetation
229 (chlorophyll), or bare soil (values around zero), whereas values below zero indicate the
230 existence of water, snow, ice and clouds.

231

232 **2.2 Database**

233 Scientific research satellite Terra (EOS AM-1) has been chosen to provide
234 necessary information to calculate NDVI in the study area. This satellite was launched
235 into orbit by NASA on December 18, 1999. MODIS (Moderate Resolution Imaging
236 Spectroradiometer) sensor aboard this satellite collects information of different
237 reflectance bands. MODIS information is organized by "products". The product used in
238 this study was MOD09A1 (LP DAAC, 2014). MOD09A1 incorporates seven frequency
239 bands: Band 1 (620-670 nm), band 2 (841-876 nm), band 3 (459-479 nm), band 4
240 (545-565 nm), 5 band (1230-1250 nm), band 6 (1628-1652 nm) and band 7 (2105-2155



241 nm). The bands used to calculate NDVI are: band 1 for red frequency and band 2 for
242 near-infrared frequency. MOD09A1 provides georeferenced images with pixel
243 resolution of 500m x 500m. This product has a mix of the best reflectance measures of
244 each pixel in an 8-days period.

245

246 Daily data from the completed station of meteorological networks were utilized
247 during the period studied (2002 – 2017). Meteorological station is located in
248 $40^{\circ}41'46''\text{N}$ $3^{\circ}45'54''\text{W}$ (elevation 1004 m a.s.l.), less than 2 km from the study area
249 (AEMET, 2017).

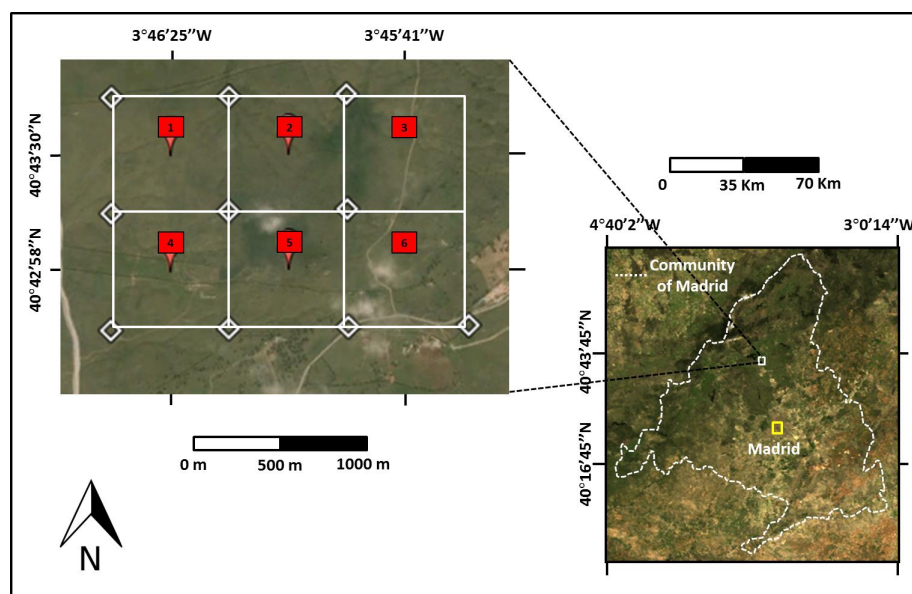
250

251 **2.3 Site description**

252 Six pixels (500m x 500m) are considered located in a pasture area at the north of
253 the Community of Madrid (Spain) between the municipalities of “Soto del Real” and
254 “Colmenar Viejo”. The study area is located between meridians $3^{\circ} 45' 00''$ and $3^{\circ} 47'$
255 $00''$ W and parallels $40^{\circ} 42' 00''$ and $40^{\circ} 44' 00''$ N approximately (see Fig. 1).

256

257



258

259 **Figure 1.** The study area is in the centre of the Iberian Peninsula (Community of Madrid). RGB
260 image of six pixels area used for case study is shown (Google Earth's and MODIS images).

261

262 The annual mean temperature ranges during the study period from 12.7°C to
263 13.8°C, and annual mean precipitation ranges from 360 to 781 mm. The stations



264 studied were identified semi-arid (annual ratio P/ET_o between 0.2 and 0.5) according
265 to the global aridity index developed by the United-Nations Convention to Combat
266 Desertification (UNEP, 1997). According to the climatic classification of Köppen (Kottke
267 et al., 2006), this area presents a continental Mediterranean climate temperate with
268 dry and temperate summer (type Csb). Temperature and precipitation of this site,
269 based on 20 years, is presented in Table 1.

270

271 Due to high soil moisture conditions, ash is the dominant tree, forming large
272 agroforestry systems ("dehesas") that are used for pasture. These are ecosystems with
273 high biodiversity.

274

275 **Table 1.** Monthly average of maximum temperature (T_{max}), average temperature (T_{avg}) and
276 minimum temperature (T_{min}) and precipitation (P).

Month	Jan	Feb	Mar	Apr	May	Jun	Jul	Aug	Sep.	Oct	Nov	Dec	Annual
T _{max} (°C)	7.1	9.3	12.7	15.4	19.5	24.6	28.6	28.1	23.7	16.8	11.1	7.4	17.0
T _{avg} (°C)	3.6	4.8	7.7	10.1	13.7	18.4	22.0	21.7	17.9	12.3	7.1	4.1	12.0
T _{min} (°C)	0.0	0.3	2.6	4.8	7.8	12.1	15.4	15.3	12.0	7.8	3.0	0.8	6.8
P (mm)	67.2	50.0	38.5	62.2	62.3	30.2	18.9	16.4	34.2	79.3	86.2	82.6	627.9

277

278 **2.4 HSL model**

279 There is no doubt that time-series of NDVI data from satellite sensors carry useful
280 information, which can be used for characterizing seasonal dynamics of vegetation
281 (Fensholt et al., 2012; Forkel et al., 2013). However, due to unfavorable atmospheric
282 conditions during the data acquisition, NDVI time-series curve often contains noise
283 (Motohka et al., 2011; Park, 2013). Although most of the NDVI data products are
284 temporally composited through maximum value compositing (MVC) method (Holben,
285 1986) to retain relatively cloud-free data, residual noise still exists in the data, which
286 will affect the accuracy of the NDVI value.

287

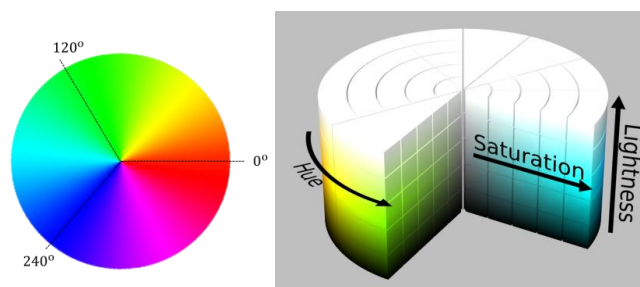
288 Therefore, usually it is necessary to reconstruct of NDVI time-series before
289 extracting information from the noisy data. There are several techniques that have
290 been applied to reduce noise and reconstruct NDVI series, a summary of these can be
291 found in Wei et al. (2016). In this study we applied a simple filtering method based on
292 the Hue-Saturation-Lightness (HSL) color model inspired by the work presented by
293 Tackenberg (2007).

294

295 HSL color model is a cylindrical representation of RGB (Red-Green-Blue) points.
296 Their components are Hue (color type), Saturation (level of color purity) and Lightness



297 (color luminosity). Hue is the angular component and it is more intuitive for humans
298 since it is directly related to the color wheel (see Fig. 2).
299



300

301

Figure 2. Colour wheel of Hue (on the left) and the HSL model (on the right).

302 Saturation is the radial component and near-zero values indicate grey colors.
303 Lightness is the axial radial versus axial component, zero lightness produces black and
304 full lightness produces white.

305

306 The NDVI series are filtered using the following HSL criteria: NDVI values are valid
307 if HSL Saturation is greater than 0.15. In this way, the values of the series that have
308 grey color correlated with pasture covered by clouds or snow are eliminated. This type
309 of filter based in HSL color space has been used on digital camera images monitoring
310 vegetation phenology (Tackenberg, 2007; Crimmins and Crimmins, 2008; Graham et
311 al., 2009). However, we have not found it in the context of remote sensing images.

312

313 **2.5 Maximum Likelihood Method (MLM)**

314 MLM estimates the set of parameters $\{\alpha, \beta, \mu, \sigma, \dots\}$ for a specific statistical
315 distribution that maximizes the “likelihood function” or the “joint density function”:

$$316 \quad L = f(\mathbf{x}, \boldsymbol{\theta}) = \prod_{i=1}^n f(x_i; \alpha, \beta, \mu, \sigma, \dots) \quad (3)$$

317 where $\mathbf{x} = (x_1, \dots, x_n)$ is the set of data, $\boldsymbol{\theta} = (\alpha, \beta, \mu, \sigma, \dots)$ is the vector of
318 parameters and $f(x_i; \alpha, \beta, \mu, \sigma, \dots)$ is the density function of the statistical model.

319 When maximization with respect to the vector of parameters is carried out, the
320 estimated parameters $(\hat{\alpha}, \hat{\beta}, \hat{\mu}, \hat{\sigma}, \dots)$ for the proposed statistical distribution are
321 obtained (Larson, 1982). Properties of estimated parameters are: invariance,
322 consistency and asymptotically unbiased.

323 In the case of a Gaussian model, the estimated statistics μ and σ are defined by
324 accurate expressions as follows:

$$\hat{\mu} = \bar{x} = \frac{1}{n} \sum_{i=1}^n x_i \quad \hat{\sigma} = s = \sqrt{\frac{1}{n} \sum_{i=1}^n (x_i - \bar{x})^2} \quad (4)$$

where $\hat{\mu}$ is the sample mean and $\hat{\sigma}$ is the sample standard deviation of the data set.

327

328 **2.6 Goodness of fit (Chi-square test)**

329 χ^2 test can be used to determine to what extent observed frequencies differ from
330 frequencies expected for a specific statistical model. The most important points of the
331 theory are briefly presented in (Cochran, 1952).

332 Let $f(x, \theta)$ be a theoretical density function of a random variable x which
333 depends on parameters $\theta = (\alpha, \beta, \mu, \sigma, \dots)$ and let x_1, \dots, x_n be a sample of x grouped
334 into k classes with n_i data per class i .

335 Firstly, the following hypothesis is set:

336 (H_0) observed data fit theoretical distribution $f(x, \theta)$.

337 Then the test statistic χ_c^2 is defined as:

$$\chi_c^2 = \sum_{i=0}^k \frac{(n_i - e_i)^2}{e_i} \quad (5)$$

339 where n_i is the number of data or observed frequency and $e_i = n \cdot P(\text{class } i)$ is the
340 expected frequency for class i . $P(\text{class } i)$ is the theoretical interval probability
341 defined for class i .

342 A level of significance is also set as:

$$\alpha = P(\text{Reject } H_0 / H_0 \text{ is true}) \quad (6)$$

344 Finally, the following decision rule is applied: "reject the theoretical distribution at
345 significance level α if:

$$\chi_c^2 = \sum_{i=0}^k \frac{(n_i - e_i)^2}{e_i} > \chi_{(k-m-1, 1-\alpha)}^2 \quad (7)$$

347 where $\chi_{(k-m-1, 1-\alpha)}^2$ is a χ^2 distribution with $k-m-1$ degrees of freedom (m is the
348 number of parameters, k is the number of classes).

349

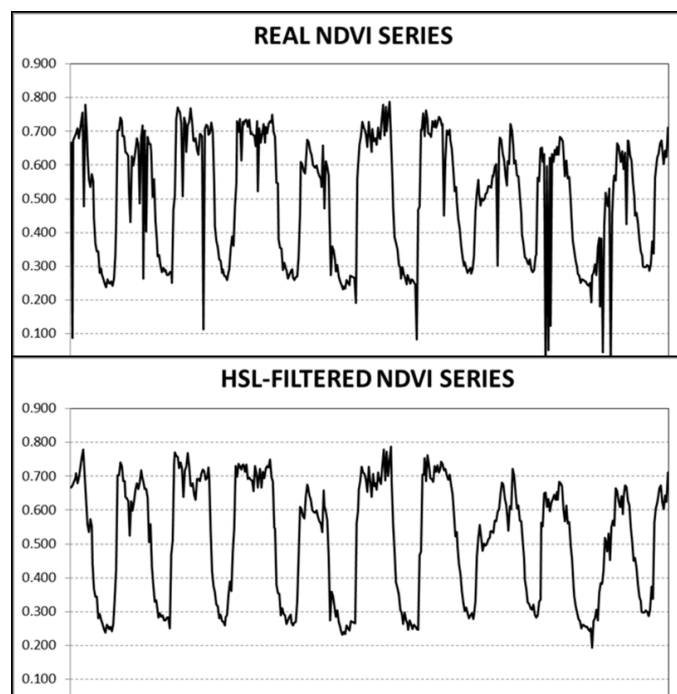
350

351 **3. Results and Discussion**

352 **3.1 HSL filtering criteria**

353 NDVI series (from 2002 to 2017) were obtained for each pixel of the study area
354 using frequency bands provided by MODIS product named MOD09A1. These series

355 contain some irregular values that can skew NDVI pattern. Therefore, the six series (six
356 pixels) were filtered using the HSL criteria. In Fig. 3 is shown an example of how HSL
357 filtering criteria works with a NDVI series.



358
359

Figure 3. HSL filtering criteria applied to a NDVI series.

360 The abrupt changes in the NDVI values, mainly observed during raining seasons
361 such as autumn and winter, are efficiently eliminated. Not to be a high computational
362 demanding method is one of the main advantages of HSL filtering method. Therefore,
363 this method will allow us to obtain more robust NDVI values to be used in the
364 statistical analysis.
365

366 **3.2 Maximum Likelihood Method (MLM) and Chi square test**

367 In this study, a random variable (RV) of NDVI values has been defined every 8 days
368 (temporal resolution of MODIS product), in such a way that 46 RVs have been obtained
369 for the whole year. In Table 2, the definition of each RV can be seen, namely, the
370 period of the year (interval) which belongs to, and the amount of available NDVI
371 samples. Each RV collects the samples coming from the six selected pixels.

372
373



374
 375

Table 2. Description of all RV defined in a year. Start - end of intervals and amount of samples are shown.

RANDOM VARIABLE	START PERIOD	END PERIOD	# SAMPLES
Interval 1	1-Jan	8-Jan	85
Interval 2	9-Jan	16-Jan	84
Interval 3	17-Jan	24-Jan	96
Interval 4	25-Jan	1-Feb	96
Interval 5	2-Feb	9-Feb	95
Interval 6	10-Feb	17-Feb	90
Interval 7	18-Feb	25-Feb	86
Interval 8	26-Feb	5-Mar	83
Interval 9	6-Mar	13-Mar	96
Interval 10	14-Mar	21-Mar	96
Interval 11	22-Mar	29-Mar	74
Interval 12	30-Mar	6-Apr	88
Interval 13	7-Apr	14-Apr	88
Interval 14	15-Apr	22-Apr	88
Interval 15	23-Apr	30-Apr	96
Interval 16	1-May	8-May	92
Interval 17	9-May	16-May	88
Interval 18	17-May	24-May	96
Interval 19	25-May	1-Jun	95
Interval 20	2-Jun	9-Jun	96
Interval 21	10-Jun	17-Jun	95
Interval 22	18-Jun	25-Jun	96
Interval 23	26-Jun	3-Jul	96
Interval 24	4-Jul	11-Jul	96
Interval 25	12-Jul	19-Jul	96
Interval 26	20-Jul	27-Jul	96
Interval 27	28-Jul	4-Aug	96
Interval 28	5-Aug	12-Aug	96
Interval 29	13-Aug	20-Aug	96
Interval 30	21-Aug	28-Aug	96
Interval 31	29-Aug	5-Sep	96
Interval 32	6-Sep	13-Sep	96
Interval 33	14-Sep	21-Sep	94
Interval 34	22-Sep	29-Sep	96
Interval 35	30-Sep	7-Oct	96
Interval 36	8-Oct	15-Oct	85
Interval 37	16-Oct	23-Oct	90
Interval 38	24-Oct	31-Oct	96
Interval 39	1-Nov	8-Nov	92
Interval 40	9-Nov	16-Nov	90
Interval 41	17-Nov	24-Nov	96
Interval 42	25-Nov	2-Dec	89
Interval 43	3-Dec	10-Dec	95
Interval 44	11-Dec	18-Dec	88
Interval 45	19-Dec	26-Dec	90
Interval 46	27-Dec	31-Dec	90

376

377

378

379

380

381

382

383

384

385

386

387

388

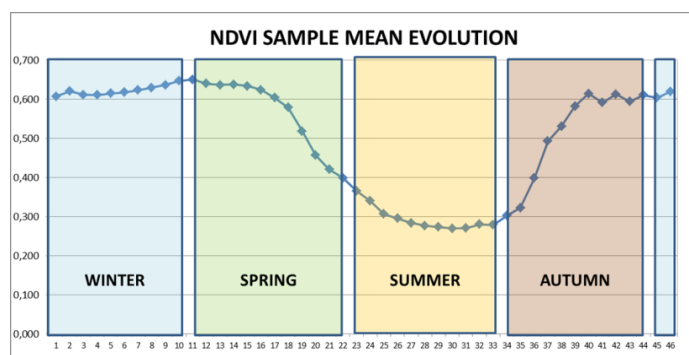
389

390

In Fig. 4, a plot with NDVI sample means of all RV with a start and end reference of the astronomical seasons is shown. The typical evolution of the NDVI along a year can be seen.



391



392

393

394

Figure 4. NDVI sample means of 46 random variables (RV) are shown as well as start and end reference of every season.

395

396

397

398

399

400

401

The observed evolution of NDVI through the different seasons is typical of the pasture in this area. The summer presents the lowest mean values which begin to increase in autumn achieving a maximum mean value of 0.60 or 0.65 during winter. In the middle of the spring NDVI decrease again, approaching the lowest mean value of 0.28 approximately.

402

403

404

405

406

Taking into account these values, dense vegetation, in this study pasture, is found from middle of October (interval 37) till the end of May (interval 19) (see Table 2). It is in this period where the precipitation concentrates (see Table 1). During the summer, the NDVI mean values are lower than 0.3 corresponding with low precipitation and high temperatures.

407

408

409

410

411

412

413

Following the work of Escribano-Rodriguez et al. (2014), there is a relationship of pasture damage and a NDVI value around 0.40. Even if the authors point out that this value is highly variable depending on the location, we can see that summer season in this case study is under this value (see Fig. 4). This can explain that “Insurances for Damaged Pasture” usually do not apply in these dates due to the arid environment (BOE, 2013).

414

415

416

417

418

419

420

421

MLM has been applied to model these 46 RV. Parameters have been calculated for 4 probability density functions (PDF) which are the candidates to be the best fit. In Table 3, a brief description is presented of these PDF candidates: Normal, Gamma, Beta and Generalized Extreme Values (GEV). To do so, the following MATLAB functions have been used: “normfit”, “gamfit”, “betafit” and “gevfit” (respectively).



422

Table 3. Candidate Probability Density Functions (PDF).

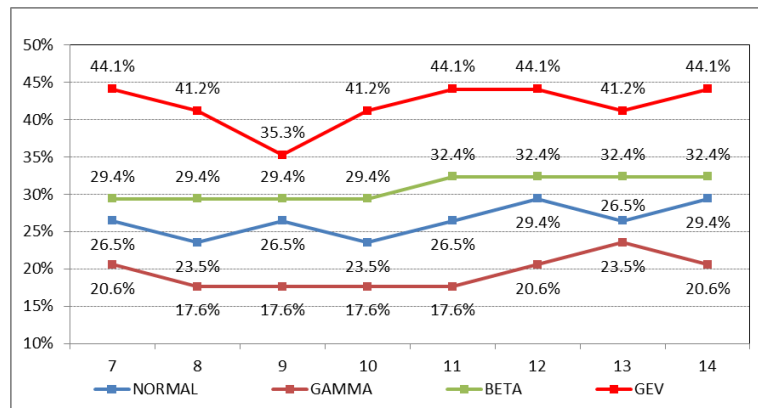
PDF NAME	PDF EXPRESSION	PDF PARAMETERS
Normal	$f(x; \mu, \sigma) = \frac{1}{\sigma\sqrt{2\pi}} e^{-\frac{1}{2}\left(\frac{x-\mu}{\sigma}\right)^2}$	$\mu \equiv$ average $\sigma \equiv$ standard deviation
Gamma	$f(x; \alpha, \beta) = \frac{1}{\beta^\alpha \Gamma(\alpha)} x^{\alpha-1} e^{-\frac{x}{\beta}}$	$\Gamma(\cdot) \equiv$ gamma function α and $\beta \equiv$ parameters
Beta	$f(x; a, b) = \frac{\Gamma(a+b)}{\Gamma(a)\Gamma(b)} x^{a-1} (1-x)^{b-1}$	$\Gamma(\cdot) \equiv$ gamma function a and $b \equiv$ parameters
Generalized Extreme Values (GEV)	$f(x; \mu, \sigma, \xi) = \frac{1}{\sigma} t(x)^{\xi+1} e^{-t(x)}$ where $t(x) = \begin{cases} \left(1 + \left(\frac{x-\mu}{\sigma}\right)\xi\right)^{-1/\xi} & \text{if } \xi \neq 0 \\ e^{-(x-\mu)/\sigma} & \text{if } \xi = 0 \end{cases}$	$\mu \in \mathbb{R} \equiv$ location param. $\sigma > 0 \equiv$ scale parameter $\xi \in \mathbb{R} \equiv$ shape parameter

423

424 To check the goodness of the fit of PDF candidates, Chi square test (χ^2 test) has
 425 been used from 7 classes to 14 classes meeting the requirement that each class has at
 426 least five observations. To calculate χ^2 , the theoretical probability defined for class i ,
 427 the following MATLAB functions have been used: “normcdf”, “gamcdf”, “betacdf” and
 428 “gevcdf”, which represent the cumulative density functions of each RV.

429

430 Twelve intervals (from 23 to 34) corresponding to months of July, August and
 431 September have been excluded of this analysis since these intervals fall into the dry
 432 season in the study area, normally not cover by any SIBI. Fig. 5 shows the percentage
 433 of intervals that fit for every PDF candidate. The number of classes used in χ^2 test is
 434 represented at X-axis (from 7 to 14 classes).



435

436 **Figure 5.** Percentage of fitted intervals for each PDF candidate (normal, gamma, beta and GEV
 437 distributions).

438

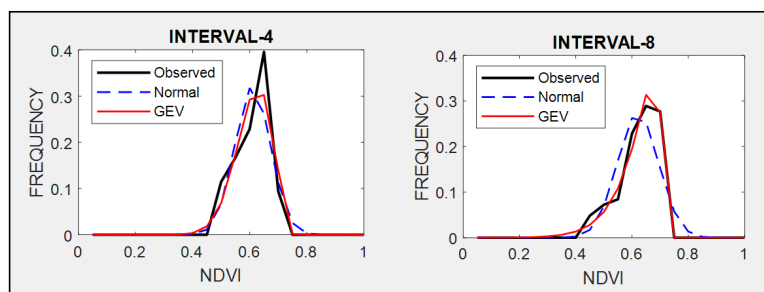


439 Fig. 5 indicates that GEV distributions explain more intervals (more than 40% for
440 the majority of different class analysis) than normal, gamma or beta distributions.
441 Therefore, the methodology applied in Turvey et al. (2012) to design an index-based
442 insurance using NDVI values will not be feasible in this case study. This one uses an
443 average and standard deviation to define a percentage of cases where NDVI value will
444 be lower than a threshold defined by normal parameters. An important different
445 between the normal distribution and the rest of the PDF used in this work is its
446 symmetry and kurtosis. Many of the observed NDVI frequency distributions present a
447 clear asymmetry and long tails in one or both sides that causes normal distribution not
448 to be the optimal fit.

449

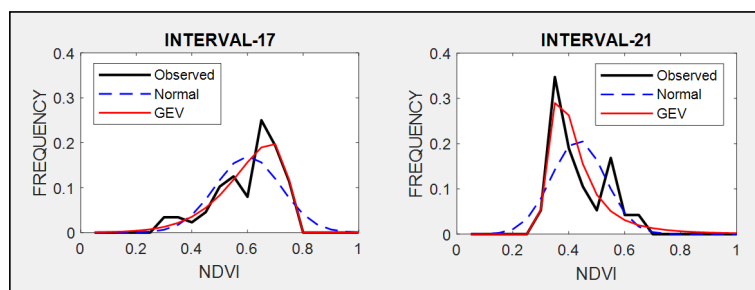
450 Table A1 at Appendix A shows the estimated parameters for each PDF and each
451 interval calculated by the MLM. These parameters will be used to compare the
452 estimated PDF with the NDVI observed values on different times through the seasons.
453 The following intervals are shown as examples of better GEV fit: interval 4 and 8 (for
454 winter, see Fig. 6), interval 17 and 21 (for spring, see Fig. 7) and interval 36 and 40 (for
455 autumn, see Fig. 8). In these plots, observed frequency is compared versus normal and
456 GEV density distributions calculated by MLM.

457



458

459 **Figure 6.** Comparison between observed NDVI frequency, GEV and normal probability density
460 functions (PDF) on two different dates. Intervals 4 and 8 are examples for winter.

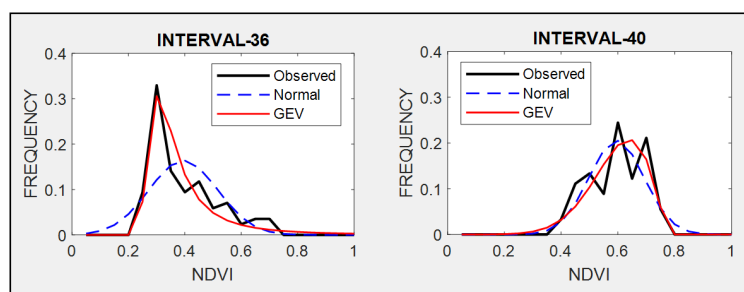


461

462 **Figure 7.** Comparison between observed NDVI frequency, GEV and Normal probability density
463 functions (PDF) on two different dates. Intervals 17 and 21 are examples for spring.



464



465

466

467

Figure 8. Comparison between observed NDVI frequency, GEV and normal probability density functions (PDF) on two different times. Intervals 36 and 41 are examples for autumn.

468

469

470

471

472

473

474

475

476

477

478

479

480

481

482

483

484

485

486

487

488

489

490

491

492

493

494

During winter (see Fig. 6) the observed NDVI distribution presents negative skewness. Then, there is a higher frequency of high NDVI values corresponding with significant precipitation. During spring an evolution in the skewness is observed passing from negative to positive, and so, the lower NDVI values become the higher probable. Finally, during autumn precipitation begins and from positive pass to negative skewness and higher NDVI values are possible. We can observe that normal distribution has no flexibility to follow this dynamic in the distributions on each time. This comparison is done in a sequential order for the whole of intervals in Figures A1, A2, A3 and A4 at Appendix A.

The more skewness and kurtosis depart from those of the normal distribution the larger the errors affecting the insurance designed based on (Turvey et al., 2012). It is an expected result as pasture scenario is quite different from the development of a crop, where normal distributions in the NDVI values are more expected. This high heterogeneity in time and space of NDVI estimated on pasture has been pointed out in several works (Martin-Sotoca et al, 2018). At the same time, more different is the observed NDVI frequency from a normal distribution less representative is the average, and so, the median becomes a more representative value.

3.3 Insurance context

The use of NDVI thresholds in damaged pasture context was presented in the introduction section, being an example of using the "Insurance for Damaged Pasture" in Spain. We have chosen this last insurance to compare the results between applying Normal and GEV distribution methodologies. In this particular case the NDVI threshold ($NDVI_{th}$) was calculated using the expression $NDVI_{th} = \mu - k \cdot \sigma$ (where μ, σ are average and standard deviation of NDVI distributions respectively, assuming the Normal hypothesis).



495

496 The probability of being below $NDVI_{th}$ (using $k = 0.7$, first damage level in the
 497 insurance) at every interval has been calculated assuming the Normal hypothesis. As it
 498 was expected, this value is always 24.2% (see third column in Table 4). The probability
 499 of being below $NDVI_{th}$ has also been calculated using GEV distributions obtained in
 500 this study. The probability obtained by GEV distributions is mostly lower than the
 501 Normal distributions in spring, autumn and winter (see Table 4) that is the working
 502 period of the insurance.

503

504 Observing where in time are localized the highest relative error in probabilities
 505 (fifth column in Table 4), in absolute values, intervals corresponding to the end of
 506 winter, second middle of spring and the beginning of autumn present errors higher
 507 than 10%. This could explain why it is in spring and autumn when more disagreements
 508 exist between farmers and insurance company in claims.

509

510 **Table 4 – First column:** time intervals of approximately 8 days along the year. **Second column:**
 511 NDVI thresholds ($NDVI_{th}$) based on a Normal distribution applying $\mu - 0.7 \times \sigma$. **Third column:**
 512 percentages of area below the $NDVI_{th}$ when Normal distributions are applied. **Fourth column:**
 513 percentages of area below the $NDVI_{th}$ when GEV distributions are applied. **Fifth column:** relative
 514 area error of GEV compared to the Normal distribution.

515

RANDOM VARIABLE	NORMAL		GEV	
	$NDVI_{th}$	Prob.	Prob.	Error (%)
Interval 1	0.535	24.20%	24.37%	0.70%
Interval 2	0.541	24.20%	23.18%	-4.21%
Interval 3	0.541	24.20%	23.27%	-3.84%
Interval 4	0.543	24.20%	23.27%	-3.84%
Interval 5	0.545	24.20%	24.17%	-0.12%
Interval 6	0.534	24.20%	21.48%	-11.24%
Interval 7	0.528	24.20%	24.01%	-0.79%
Interval 8	0.546	24.20%	20.70%	-14.46%
Interval 9	0.555	24.20%	21.30%	-11.98%
Interval 10	0.561	24.20%	22.28%	-7.93%
Interval 11	0.567	24.20%	23.49%	-2.93%
Interval 12	0.572	24.20%	23.75%	-1.86%
Interval 13	0.571	24.20%	23.20%	-4.13%
Interval 14	0.570	24.20%	24.29%	0.37%
Interval 15	0.571	24.20%	23.47%	-3.02%
Interval 16	0.560	24.20%	23.26%	-3.88%



Interval 17	0.495	24.20%	21.29%	-12.02%
Interval 18	0.484	24.20%	21.58%	-10.83%
Interval 19	0.442	24.20%	23.06%	-4.71%
Interval 20	0.381	24.20%	27.20%	12.40%
Interval 21	0.342	24.20%	29.46%	21.74%
Interval 22	0.323	24.20%	28.84%	19.17%
Interval 35	0.257	24.20%	18.98%	-21.57%
Interval 36	0.285	24.20%	28.57%	18.06%
Interval 37	0.333	24.20%	25.90%	7.02%
Interval 38	0.398	24.20%	24.27%	0.29%
Interval 39	0.454	24.20%	23.79%	-1.69%
Interval 40	0.503	24.20%	22.81%	-5.74%
Interval 41	0.491	24.20%	23.23%	-4.01%
Interval 42	0.517	24.20%	24.66%	1.90%
Interval 43	0.507	24.20%	23.13%	-4.42%
Interval 44	0.514	24.20%	23.49%	-2.93%
Interval 45	0.515	24.20%	23.70%	-2.07%
Interval 46	0.509	24.20%	23.33%	-3.60%

516

517 In Table 4, Normal $NDVI_{th}$ have been used to calculate the probability in GEV
 518 distributions. An alternative calculation can be the use of normal probability (24.2%) to
 519 calculate new $NDVI_{th}$ based on GEV (see Table 5). It can be seen that new $NDVI_{th}$
 520 obtained by GEV distributions are mostly upper than thresholds using Normal
 521 distributions in spring, autumn and winter. Considering these results we find that
 522 damage thresholds calculated by GEV methodology are mostly above that one's
 523 calculated by Normal methodology.

524 Again, intervals corresponding to the end of winter, second middle of spring and the
 525 beginning of autumn present $NDVI_{th}$ relative errors higher than 1% in absolute values
 526 (fourth column in Table 5).

527

528 **Table 5 - First column:** time intervals of approximately 8 days along the year. **Second column:** NDVI
 529 thresholds ($NDVI_{th}$) based on a Normal distribution (Normal) applying $\mu - 0.7 \times \sigma$. **Third column:**
 530 $NDVI_{th}$ based on a GEV distribution (GEV) using 24.2% as the area below the $NDVI_{th}$. **Fourth**
 531 **column:** relative $NDVI_{th}$ error of GEV compared to the Normal distribution.

532

533



RANDOM VARIABLE	NDVI _{Th}		Error (%)
	Normal	GEV	
Interval 1	0.535	0.534	-0,19%
Interval 2	0.541	0.543	0,37%
Interval 3	0.541	0.543	0,37%
Interval 4	0.543	0.545	0,37%
Interval 5	0.545	0.545	0,00%
Interval 6	0.534	0.543	1,69%
Interval 7	0.528	0.528	0,00%
Interval 8	0.546	0.558	2,20%
Interval 9	0.555	0.563	1,44%
Interval 10	0.561	0.567	1,07%
Interval 11	0.567	0.569	0,35%
Interval 12	0.572	0.574	0,35%
Interval 13	0.571	0.574	0,53%
Interval 14	0.570	0.569	-0,18%
Interval 15	0.571	0.573	0,35%
Interval 16	0.560	0.563	0,54%
Interval 17	0.495	0.510	3,03%
Interval 18	0.484	0.498	2,89%
Interval 19	0.442	0.447	1,13%
Interval 20	0.381	0.374	-1,84%
Interval 21	0.342	0.334	-2,34%
Interval 22	0.323	0.318	-1,55%
Interval 35	0.257	0.262	1,95%
Interval 36	0.285	0.278	-2,46%
Interval 37	0.333	0.327	-1,80%
Interval 38	0.398	0.398	0,00%
Interval 39	0.454	0.455	0,22%
Interval 40	0.503	0.508	0,99%
Interval 41	0.491	0.494	0,61%
Interval 42	0.517	0.516	-0,19%
Interval 43	0.507	0.510	0,59%
Interval 44	0.514	0.516	0,39%
Interval 45	0.515	0.516	0,19%
Interval 46	0.509	0.511	0,39%

534

535 **4. Conclusions**

536 According to the results obtained in the study area using MLM and χ^2 test, it can
 537 be concluded that normal distributions are not the best fit to the NDVI observations,
 538 and GEV distributions provide a better approximation.

539



540 The difference between Normal and GEV assumption is more evident in the
541 transition from winter to summer (spring), where NDVI values decrease, and then from
542 summer to winter (autumn) presenting the opposite behavior of increasing NDVI
543 values. In both periods asymmetrical distributions were found, negative skewness for
544 the spring transition and positive skewness for the autumn transition. During both
545 periods the variability in precipitation and temperatures were higher in this location.

546

547 We have found differences if GEV assumption is selected instead of the Normal
548 one when defining damaged pasture thresholds ($NDVI_{th}$). The use of these different
549 assumptions should be taken into account in future insurance implementations due to
550 the important consequences of supposing a damage event or not. We propose the use
551 of percentiles in experimental NDVI distributions instead of average and standard
552 deviation, typically of normal distributions, to calculate new $NDVI_{th}$.

553

554

555 **Acknowledgements**

556 This research has been partially supported by funding from MINECO under contract
557 No. MTM2015-63914-P and CICYT PCIN-2014-080.

558



559 **Appendix A**

560

561

Table A1 - Maximum Likelihood parameters calculated for 4 PDF.

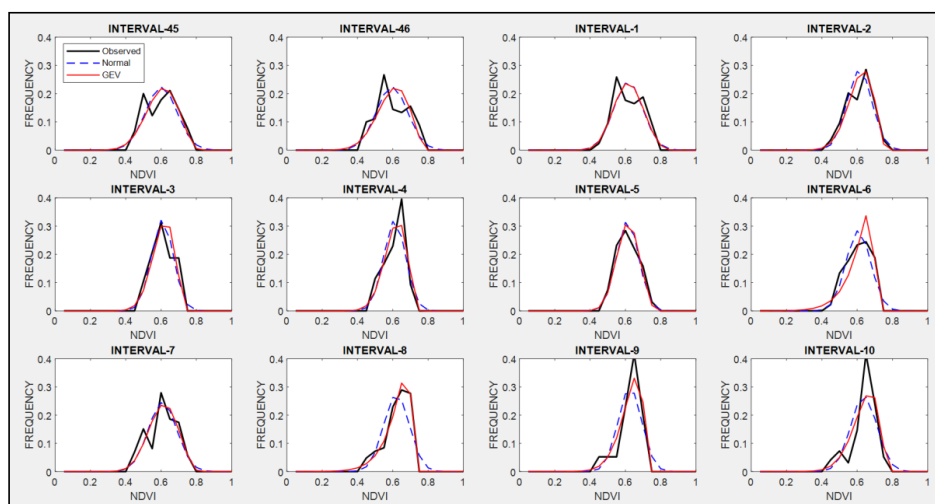
RANDOM VARIABLE	NORMAL		GAMMA		BETA		GEV		
	μ	σ	α	β	a	b	μ	σ	ξ
Interval 1	0.591	0.081	53.31	0.011	21.45	14.82	0.563	0.080	-0.297
Interval 2	0.589	0.069	71.14	0.008	30.62	21.40	0.571	0.073	-0.477
Interval 3	0.583	0.060	94.15	0.006	39.56	28.34	0.567	0.063	-0.457
Interval 4	0.585	0.060	91.88	0.006	39.58	28.05	0.570	0.064	-0.468
Interval 5	0.588	0.061	93.92	0.006	38.83	27.25	0.568	0.061	-0.340
Interval 6	0.582	0.068	70.28	0.008	30.67	22.05	0.577	0.083	-0.846
Interval 7	0.584	0.080	52.52	0.011	22.16	15.82	0.559	0.082	-0.366
Interval 8	0.596	0.071	65.37	0.009	28.89	19.59	0.591	0.081	-0.833
Interval 9	0.601	0.066	76.02	0.008	34.31	22.84	0.590	0.070	-0.652
Interval 10	0.613	0.073	63.83	0.010	27.80	17.62	0.598	0.079	-0.572
Interval 11	0.621	0.078	58.72	0.011	24.33	14.86	0.600	0.083	-0.451
Interval 12	0.624	0.073	68.33	0.009	28.01	16.94	0.603	0.078	-0.431
Interval 13	0.624	0.075	66.22	0.009	26.23	15.85	0.604	0.080	-0.476
Interval 14	0.631	0.088	50.23	0.013	18.71	10.92	0.603	0.090	-0.342
Interval 15	0.630	0.084	53.60	0.012	21.17	12.45	0.607	0.089	-0.448
Interval 16	0.627	0.096	38.75	0.016	16.08	9.59	0.602	0.103	-0.474
Interval 17	0.577	0.117	20.47	0.028	10.24	7.58	0.560	0.127	-0.692
Interval 18	0.568	0.120	20.52	0.028	9.71	7.42	0.552	0.136	-0.718
Interval 19	0.523	0.116	19.46	0.027	9.52	8.68	0.495	0.125	-0.493
Interval 20	0.452	0.101	20.99	0.022	10.98	13.31	0.401	0.077	0.078
Interval 21	0.409	0.095	19.94	0.021	11.18	16.13	0.354	0.060	0.325
Interval 22	0.379	0.080	24.66	0.015	14.41	23.52	0.333	0.046	0.385
Interval 23	0.353	0.073	26.54	0.013	15.85	29.01	0.311	0.036	0.456
Interval 24	0.328	0.056	38.36	0.009	24.22	49.65	0.298	0.033	0.287
Interval 25	0.305	0.044	53.52	0.006	35.62	81.20	0.282	0.028	0.210
Interval 26	0.298	0.034	78.93	0.004	54.47	128.55	0.283	0.029	-0.064
Interval 27	0.289	0.026	126.85	0.002	88.33	217.15	0.278	0.021	-0.030
Interval 28	0.282	0.022	166.17	0.002	119.50	305.03	0.274	0.022	-0.322
Interval 29	0.278	0.021	179.09	0.002	127.93	332.63	0.269	0.018	-0.085
Interval 30	0.273	0.019	203.11	0.001	147.67	393.21	0.266	0.019	-0.247
Interval 31	0.272	0.022	166.83	0.002	120.11	321.95	0.262	0.018	-0.059
Interval 32	0.280	0.034	75.63	0.004	52.36	134.30	0.264	0.023	0.118
Interval 33	0.285	0.034	82.05	0.004	54.90	137.68	0.270	0.020	0.122
Interval 34	0.295	0.057	33.26	0.009	21.15	50.37	0.268	0.024	0.363
Interval 35	0.312	0.079	19.70	0.016	11.83	25.94	0.275	0.038	0.300
Interval 36	0.369	0.121	10.81	0.034	6.11	10.33	0.298	0.063	0.480
Interval 37	0.432	0.141	9.45	0.046	5.21	6.81	0.370	0.120	-0.080



Interval 38	0.487	0.128	13.88	0.035	7.25	7.63	0.445	0.127	-0.321
Interval 39	0.529	0.107	23.56	0.022	11.39	10.16	0.497	0.110	-0.390
Interval 40	0.570	0.096	34.02	0.017	15.10	11.40	0.548	0.105	-0.533
Interval 41	0.554	0.090	36.42	0.015	16.90	13.64	0.531	0.096	-0.471
Interval 42	0.583	0.095	37.29	0.016	15.56	11.11	0.551	0.094	-0.295
Interval 43	0.574	0.097	34.27	0.017	14.93	11.07	0.550	0.103	-0.482
Interval 44	0.572	0.083	47.13	0.012	20.40	15.26	0.549	0.086	-0.425
Interval 45	0.576	0.088	42.59	0.014	18.17	13.36	0.550	0.090	-0.396
Interval 46	0.570	0.088	41.98	0.014	18.11	13.66	0.546	0.092	-0.445

562

563



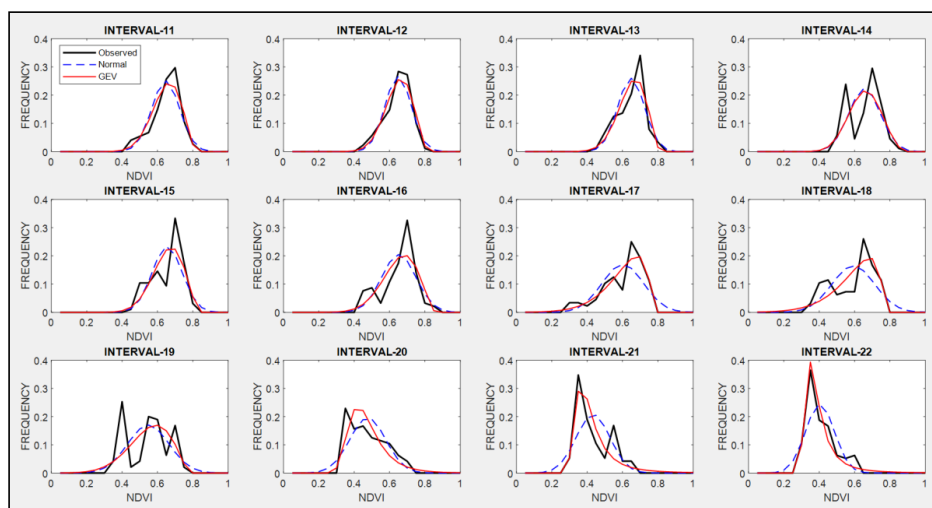
564

565

566

Figure A1. Observed NDVI, GEV and Normal probability density functions (PDF) from interval 45 to interval 10 (from 19 December to 21 March) representing Winter.

567



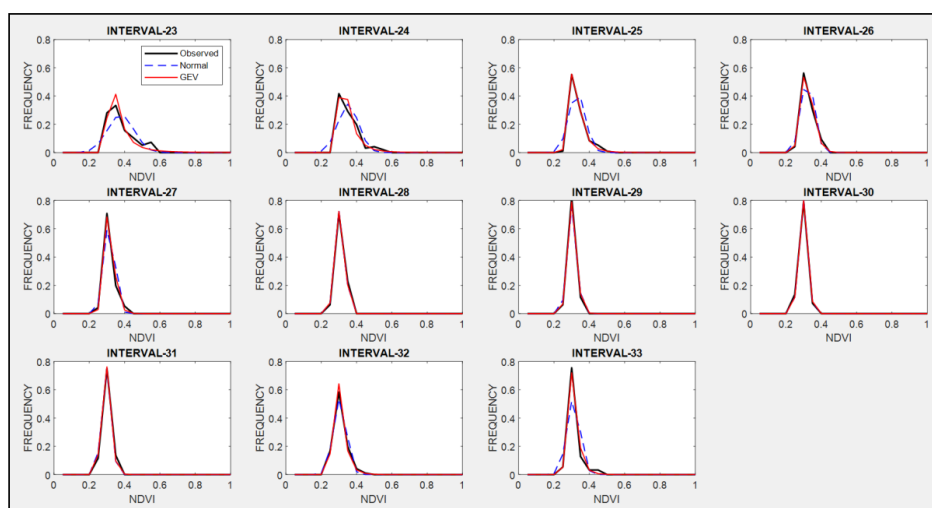
568

569

570

Figure A2. Observed NDVI, GEV and Normal probability density functions (PDF) from interval 11 to interval 22 (from 22 March to 25 June) representing Spring.

571



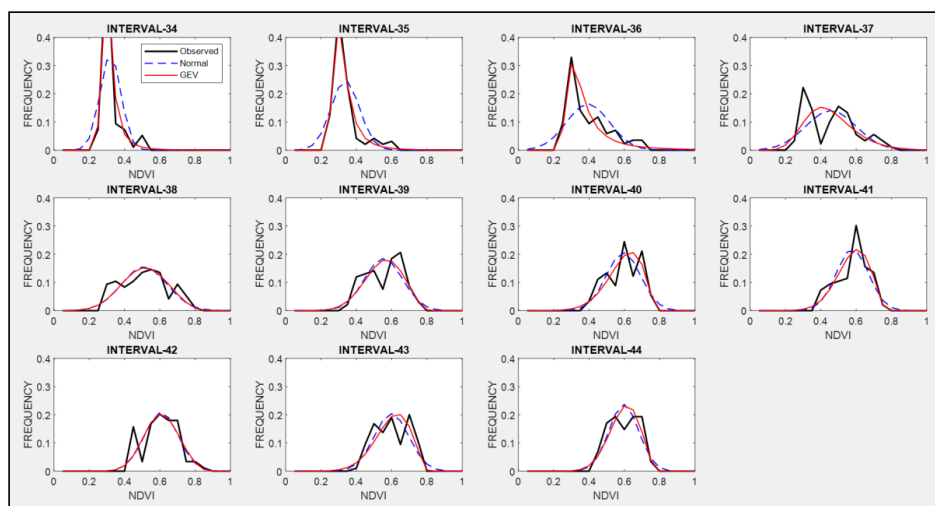
572

573

574

Figure A3. Observed NDVI, GEV and Normal probability density functions (PDFs) from interval 23 to interval 33 (from 26 June to 21 September) representing Summer.

575



576

577

578

Figure A4. Observed NDVI, GEV and Normal PDFs from interval 34 to interval 44 (from 22 September to 18 December) representing Autumn.

579

580 **References**

581

582 Agencia Estatal de Meteorología (AEMET). Available at: www.aemet.es. 2017.

583 Al-Bakri, J.T.; Taylor, J.C.: Application of NOAA AVHRR for monitoring vegetation
584 conditions and biomass in Jordan, *J. Arid Environ*, 54, 579–593, 2003.

585 Bailey, S.: The Impact of Cash Transfers on Food Consumption in Humanitarian Settings:
586 A review of evidence, Study for the Canadian Foodgrains Bank, May 2013.

587 Boletín Oficial del Estado (BOE, 6638 - Orden AAA/1129/2013. Nº 145, III, p-46077.
588 2013.

589 Cochran, William G.: The Chi-square Test of Goodness of Fit, *Annals of Mathematical*
590 *Statistics*. 23: 315–345, 1952.

591 Crimmins, M.A.; Crimmins T. M.: Monitoring plant phenology using digital repeat
592 photography, *Environ. Manage*, 41, 949-958, 2008.

593 Dalezios, N. R.; Blanta, A.; Spyropoulos, N.V.; Tarquis A.M.: Risk identification of
594 agricultural drought for sustainable Agroecosystems, *Nat. Hazards Earth Syst. Sci.*,
595 14, 2435–2448, 2014.

596 Dalezios, N.R.: The Role of Remotely Sensed Vegetation Indices in Contemporary
597 Agrometeorology. Invited paper in Honorary Special Volume in memory of late
598 Prof. A. Flokas. Publisher: Hellenic Meteorological Association, 33-44, 2013.

599 De Leeuw, J.; Vrieling, A.; Shee, A.; Atzberger, C.; Hadgu, K.M.; Biradar, C.M.;
600 Humphrey Keah, H.; Turvey, C.: The Potential and Uptake of Remote Sensing in
601 Insurance: A Review, *Remote Sens.*, 6(11), 10888-10912, 2014.

602 Escribano Rodríguez, J. Agustín; Díaz-Ambrona, Carlos Gregorio H.; and Tarquis Alfonso,
603 Ana María: Selection of vegetation indices to estimate pasture production in
604 Dehesas, *PASTOS*, 44(2), 6-18, 2014.

605 Fensholt, R.; Proud, S.R.: Evaluation of earth observation based global long term
606 vegetation trends - comparing GIMMS and MODIS global NDVI time series. *Remote*
607 *Sens. Environ.*, 119, 131–147, 2012.

608 Flynn E.S.: Using NDVI as a pasture management tool. Master Thesis, University of
609 Kentucky, 2006.

610 Forkel, M.; Carvalhais, N.; Verbesselt, J.; Mahecha, M.D.; Neigh, C.S.; Reichstein, M.:
611 Trend change detection in NDVI time series: effects of inter-annual variability and
612 methodology. *Remote Sens.*, 5, 2113–2144, 2013.

613 Fuller, D.O.: Trends in NDVI time series and their relation to rangeland and crop
614 production in Senegal, 1987–1993, *Int. J. Remote Sens.*, 19, 2013–2018, 1998.

615 Gomme, R.; Kayitakire F. (eds.): The challenges of index-based insurance for food
616 security in developing countries. Proceedings, Technical Workshop, JRC, Ispra, 2-3
617 May 2012. Publisher: JRC-EC, p. 276, 2013.

618 Gouveia, C., Trigo, R. M., and Da Camara, C. C.: Drought and vegetation stress
619 monitoring in Portugal using satellite data, *Nat. Hazards Earth Syst. Sci.*, 9, 185-195,
620 2009.

- 621 Goward, S.N.; Tucker, C.J.; Dye, D.G.: North-American vegetation patterns observed
622 with the NOAA-7 advanced very high-resolution radiometer. *Vegetation*, 64, 3–14,
623 1985.
- 624 Graham, E. A.; Yuen, E. M.; Robertson, G. F.; Kaiser, W. J.; Hamilton, M. P.; Rundel, P.
625 W.: Budburst and leaf area expansion measured with a novel mobile camera
626 system and simple color thresholding, *Environ. Exp. Bot.*, 65, 238-244, 2009.
- 627 Hobbs, T.J.: The use of NOAA-AVHRR NDVI data to assess herbage production in the
628 arid rangelands of central Australia, *Int. J. Remote Sens.*, 16, 1289–1302, 1995.
- 629 Holben, B. N.: Characteristics of maximum-value composite images from temporal
630 AVHRR data, *Int. J. Remote Sens.*, 7, 1417–1434, 1986.
- 631 Kottek, M.; Grieser, J.; Beck, C.; Rudolf, B.; Rubel, F.: World Map of the Köppen-Geiger
632 climate classification updated, *Meteorologische Zeitschrift*, 15, 259-263, 2006.
- 633 Kundu, A.; Dwivedi, S.; Dutta, D.: Monitoring the vegetation health over India during
634 contrasting monsoon years using satellite remote sensing indices, *Arab J Geosci.*, 9,
635 144, 2016.
- 636 Land Processes Distributed Active Archive Center (LP DAAC): Surface Reflectance 8-Day
637 L3 Global 500m. NASA and USGS. Available
638 at:https://lpdaac.usgs.gov/products/modis_products_Table/mod09a1. 2014.
- 639 Larson, H. J.: *Introduction to Probability Theory and Statistical Inference* (3rd edition).
640 New York, John Wiley and Sons, 1982.
- 641 Leblois, A.: Weather index-based insurance in a cash crop regulated sector: ex ante
642 evaluation for cotton producers in Cameroon. Paper presented at the JRC/IRI
643 workshop on The Challenges of Index-Based Insurance for Food Security in
644 Developing Countries, Ispra, 2-3, May, 2012.
- 645 Lovejoy, S.; Tarquis, A.M.; Gaonac’h, H.; Schertzer, D.: Single and Multiscale remote
646 sensing techniques, multifractals and MODIS derived vegetation and soil moisture.
647 *Vadose Zone J.*, 7, 533-546, 2008.
- 648 Maples, J.G.; Brorsen, B.W.; Biermachs, J.T.: The rainfall Index Annual Forage pilot
649 program as a risk management tool for cool-season forage. *J. Agr. Appl Econ*, 48(1),
650 29–51, 2016.
- 651 Martin-Sotoca, J.J.; Saa-Requejo, A.; Orondo J.B.; Tarquis, A.M.: Singularity maps
652 applied to a vegetation index. *Bio. Eng.* 168, 42-53, 2018.
- 653 Motohka, T.; Nasahara, K.N.; Murakami, K.; Nagai, S.: Evaluation of sub-pixel cloud
654 noises on MODIS daily spectral indices based on in situ measurements, *Remote*
655 *Sens.*, 3, 1644–1662, 2011.
- 656 Niemeyer, S.: New drought indices. First Int. Conf. on Drought Management: Scientific
657 and Technological Innovations, Zaragoza, Spain. Joint Research Centre of the
658 European Commission. Available online at
659 <http://www.iamz.ciheam.org/medroplan/zaragoza2008/Sequia2008/Session3/S.Niemeyer.pdf>. 2008
660



- 661 Ortega-Farias, S.; Ortega-Salazar, S.; Poblete, T.; Kilic, A.; Allen, R.; Poblete-Echeverría,
662 C.; Ahumada-Orellana, L.; Zuñiga, M.; Sepúlveda, D. Estimation of Energy Balance
663 Components over a Drip-Irrigated Olive Orchard Using Thermal and Multispectral
664 Cameras Placed on a Helicopter-Based Unmanned Aerial Vehicle (UAV), *Remote*
665 *Sens.*, 8, 638, pp 18, 2016.
- 666 Park, S.: Cloud and cloud shadow effects on the MODIS vegetation index composites of
667 the Korean Peninsula, *Int. J. Remote Sens.*, 34, 1234–1247, 2013.
- 668 Rao, K. N.: Index based Crop Insurance, *Agric. Agric. Sci. Proc.*, 1, 193–203, 2010.
- 669 Roumiguié, A.; Sigel, G.; Poilvé, H.; Bouchard, B.; Vrieling, A.; Jacquin, A. Insuring
670 forage through satellites: testing alternative indices against grassland production
671 estimates for France, *Int. J. Remote Sens.*, 38, 1912–1939, 2017.
- 672 Roumiguié, A.; Jacquin, A.; Sigel, G.; Poilvé, H.; Lepoivre, B.; Hagolle, O.: Development
673 of an index-based insurance product: validation of a forage production index
674 derived from medium spatial resolution fCover time series, *GIScience Remote*
675 *Sens.*, 52, 94–113, 2015.
- 676 Tackenberg, Oliver: A New Method for Non-destructive Measurement of Biomass,
677 Growth Rates, Vertical Biomass Distribution and Dry Matter Content Based on
678 Digital Image Analysis, *Annals of Botany*, 99(4), 777–783, 2007.
- 679 Turvey, C.G.; Mcaurin, M.K.: Applicability of the Normalized Difference Vegetation
680 Index (NDVI) in Index-Based Crop Insurance Design, *Am. Meorol. Soc.*, 4, 271–284,
681 2012.
- 682 UNEP Word Atlas of Desertification. Second Ed. United Nations Environment Programme,
683 Nairobi, 1997.
- 684 USDA. U.S. Department of Agriculture, Federal Crop Insurance Corporation, Risk
685 Management Agency: Rainfall Index Plan Annual Forage Crop Provisions. 16- RI-AF.
686 <http://www.rma.usda.gov/policies/ri-vi/2015/16riaf.pdf> 2013 (Accessed March 1,
687 2018).
- 688 Wei, W.; Wu, W.; Li, Z.; Yang, P.; Qingbo Zhou, Q.: Selecting the Optimal NDVI
689 Time-Series Reconstruction Technique for Crop Phenology Detection, *Intell. Autom.*
690 *Soft. Co.* 22, 237–247, 2016.
- 691
692
693